

Biomarker and stable carbon isotope analyses of sedimentary organic matter from Lake Tswaing: evidence for deglacial wetness and early Holocene drought from South Africa

I. Kristen · H. Wilkes · A. Vieth · K.-G. Zink ·
B. Plessen · J. Thorpe · T. C. Partridge ·
H. Oberhänsli

Received: 15 July 2008 / Accepted: 19 October 2009 / Published online: 17 November 2009
© Springer Science+Business Media B.V. 2009

Abstract Comparing the organic matter (OM) composition of modern and past lake sediments contributes to the understanding of changes in lacustrine environments over time. We investigate modern plant and lake-water samples as well as modern and ancient sediment samples from the Tswaing Crater in South Africa using biomarker and stable carbon isotope analyses on bulk OM and specific biomarker compounds. The characteristic molecular markers for higher land plants (predominantly C₃-type deciduous angiosperms) in Lake Tswaing are long-chain *n*-alkanes (*n*-C_{27–33}), *n*-alkanoles (*n*-C₂₈₊₃₀), stigmasterol, β -sitosterol, β -amyirin,

α -amyirin and lupeol. The C₁₇ *n*-alkane, tetrahymanol, gammaceran-3-one and C₂₉ sterols dominate the lipid fraction of autochthonously produced OM. By comparing stable carbon isotope analyses on bulk OM and the characteristic biomarkers, we follow the modern carbon cycle in the crater environment and find indications for methanotrophic activity in the lake from isotopically depleted moretene. A comparative study of core sediments reveals changes in the terrestrial (C₃ versus C₄) and aquatic bioproductivity and allows insights into the variability of the carbon cycle under the influence of changing climatic conditions for the time from the end of the last glacial (Termination I) to the late Holocene, ca. 14,000–2,000 calibrated years before present (years BP). The most pronounced changes occur in the

Electronic supplementary material The online version of this article (doi:10.1007/s10933-009-9393-9) contains supplementary material, which is available to authorized users.

I. Kristen (✉) · H. Wilkes · A. Vieth ·
K.-G. Zink · B. Plessen · H. Oberhänsli
Helmholtz-Zentrum Potsdam, Deutsches
GeoForschungsZentrum GFZ, Telegrafenberg,
14473 Potsdam, Germany
e-mail: iris_kristen@yahoo.com

H. Wilkes
e-mail: wilkes@gfz-potsdam.de

A. Vieth
e-mail: vieth@gfz-potsdam.de

B. Plessen
e-mail: birgit@gfz-potsdam.de

H. Oberhänsli
e-mail: oberh@gfz-potsdam.de

K.-G. Zink
GNS Science, PO Box 30368, Lower Hutt 5040,
New Zealand
e-mail: k.zink@gns.cri.nz

J. Thorpe
Department of Geography, University College London,
26 Bedford Way, London WC1H 0AP, Great Britain
e-mail: jo_thorpe@yahoo.com

T. C. Partridge
Climate Research Group, University of Witwatersrand,
Private Bag 3, Wits 2050, South Africa
e-mail: tcp@iafrica.com

aquatic realm after ca. 10,000 years BP when our results imply climate swings from more humid to more arid and after 7,500 years BP to gradually more humid conditions again, which can be related to a shift in the position of the Inter-Tropical Convergence Zone or to changes in the tropical atmosphere–ocean interaction. Long-chain alkenones (LCAs) have been identified in ancient lake sediments from Africa for the first time. They occur in samples older than 7,500 years BP and their distribution (dominance of C₃₈ and of tri- over tetra-unsaturated LCAs) is distinctly different from other published records suggesting a to date unknown source organism.

Keywords Termination I · Compound-specific stable carbon isotopes · Cyanobacteria · Alkenones · Methanotrophy · Precipitation

Introduction

The sedimentary record from Lake Tswaing (formerly “Pretoria Saltpan”) has been studied for about 20 years. Timothy C. Partridge was the first to discover the potential of this record as a climate archive and initiated the first scientific coring campaign in 1988/1989. The work focused predominantly on inorganic variables (grain size, mineralogy, geochemistry) and provided several new southern African palaeoclimate studies (Partridge 1999). Pollen, although absent over wide parts of the profile, was the only investigated organic variable besides diatoms (Scott 1999). The characterisation of lacustrine sedimentary organic matter (OM), however, can provide a variety of insights into past ecosystems and environments, such as into bioproductivity, circulation conditions, and the composition of the surrounding vegetation. Stable carbon isotope data from bulk and specific sedimentary OM can be used for addressing processes relevant for the carbon cycle of individual ecosystems. They can provide insight into carbon assimilation of land plants (C3 versus C4), the carbon source for aquatic organisms (e.g. dissolved CO₂, HCO₃[−], or methane) and influences on the respective carbon source, such as changes in atmospheric CO₂ levels, temperature, nutrient availability and bioproductivity, or intensity of recycling (Leng et al. 2005).

In a previous study, organic petrology and Rock–Eval pyrolysis were used to investigate the nature and origin of the OM in Lake Tswaing sediments over the last 200,000 years and elucidated intervals of good OM preservation with high input from autochthonous sources (filamentous algae or cyanobacteria and *Botryococcus*) (Kristen et al. 2007). In this study we report on detailed biomarker analyses of the soluble OM to understand changes in the ecosystem of the Tswaing Crater since the end of the last glacial. The combination of biomarker analyses, analyses of stable carbon isotope ratios of bulk OM, and compound-specific stable carbon isotope ratios of plant and sediment material allow a comprehensive description of the present-day ecosystem of the Tswaing Crater and its carbon cycle. With the subsequent investigation of a sedimentary sequence covering the time ca. 14,000–2,000 years BP, we aim to trace changes in the past ecosystem and the carbon cycle and to evaluate variations in the light of regional and global climate change.

Similar approaches with a direct comparison of modern and past ecosystems are rare for Africa. Yet, with increasing numbers of climate studies, the number of studies with contradictory interpretations also increases (Castañeda et al. 2007; de Mesmay 2008), highlighting the need for a solid understanding of the investigated variables and the specific conditions at the investigated site. Organic geochemical studies from Africa to date have focussed predominantly on past vegetation and palaeoclimate changes, on tropical Africa, and on the last glacial/interglacial cycle. Investigations on the lipid content (*n*-alkanes, *n*-alkanols, *n*-alkanoic acids) and the compound-specific or bulk organic stable carbon isotopic composition (Ficken et al. 1998; Street-Perrott et al. 2004), combined with investigations on pollen and grass cuticles (Ficken et al. 2002; Wooller et al. 2003) have revealed that during the last glacial period C4 grasses dominated over C3 plants in the neighbourhood of lakes at Mount Kenya (East Africa). Opposite conditions prevailed during the early Holocene. This vegetation change is interpreted as a response to the combination of lower atmospheric CO₂-concentrations and reduced precipitation during glacial times and vice versa during the early Holocene. Similar hydrological conditions are reported from Lake Victoria (Talbot and Lærdal 2000). The latter experienced several abrupt lake-level changes from the last glacial

maximum (LGM), when the lake was desiccated, to more stable Holocene conditions. Most of the referred studies on biomarkers assume the general validity of published data to assign specific OM sources, variable OM input and depositional conditions. However, lakes are individual systems with specific geological, limnological, environmental and climatic conditions and responses, which influence the nature of the OM. Accordingly, this paper deals with a detailed study of the present-day ecosystem of the Tswaing Crater, and we use our data to evaluate changes recorded in the sedimentary OM spanning the time ca. 14,000–2,000 years BP. Special attention is given to the influence of climate on the ecosystem variability.

Study site

The 1.13-km-wide crater Tswaing is located ~40 km northwest of Pretoria at an altitude of 1,045 m above sea level (asl). The crater was formed in granitic bedrock by a meteorite impact, which has been dated to 220 ± 52 k years BP using fission-track dating (Partridge 1999). The crater walls reach 119 m above the crater floor and 60 m above the adjacent surface. They form a closed basin with no surface inflow or outflow and a lake in the centre. At present, the lake is 2–3 m deep, alkaline with a pH around 10, and hypersaline (up to 250–300‰ in bottom waters). Located in the austral summer rainfall zone, it receives rainfall and groundwater inflow between October and April ($400\text{--}750 \text{ mm a}^{-1}$) when the inter-tropical convergence zone (ITCZ) reaches its southernmost position. During winter time the climate is dry, and according to monitoring data collected

during 28 months, the lake loses 30% of its volume (Ashton 1999). The high salinity causes the water body to be constantly stratified and thus anoxic below 50 cm water depth. During night-time, oxygen-deficiency prevails throughout the whole water column (Ashton 1999). These conditions, together with the high alkalinity of the lake water body, effectuate microbes and cyanobacteria to be the dominant organisms. A few diatom species inhabit areas where fresh groundwater seeps into the lake. This groundwater inflow, together with rainfall, represents the natural source of freshwater. Artesian boreholes that reach down to sandy aquifers below the carbonaceous lacustrine facies provide additional leak inflow since the 1970s (Ashton 1999). Monthly mean maximum air temperatures in the region range from 14.2 to 35.2°C, and mean minimum temperatures range from 3.6 to 15.6°C (Ashton 1999). The vegetation around the crater today is classified as Mixed and Sourish-Mixed Bushveld assemblages and consists of grassland mixed with deciduous trees and shrubs dominated by *Acacia* and *Combretum* species (Fig. 1). While trees and bushes are predominantly C3 plants, grasses in this dry, summer-rainfall area are dominated by C4 species (Scott 2002).

Materials and methods

Sample preparation, extraction and fraction separation

During May 2005 and April 2006 we sampled the dominant plant species around the crater lake. We

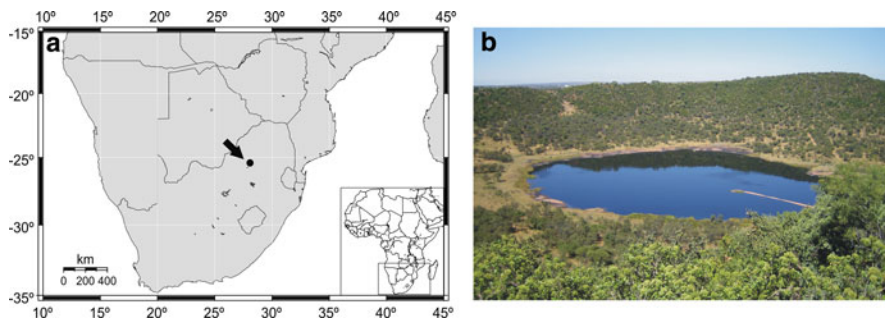


Fig. 1 **a** Map of southern Africa with the location of Lake Tswaing (arrow, $25^{\circ}24'30''\text{S}$, $28^{\circ}04'59''\text{E}$); **b** view towards the south across the Tswaing Crater in April 2006 with present-day vegetation. Note the change in the dominant species of trees/

bushes app. half way up the slope: *Acacia* species dominate the lower slope, *Spirostachys* and *Combretum* dominate the upper slope, grasses and reeds (*Typha* and *Cyperaceae*) along the shore (T. C. Partridge, pers. commun.)

also sampled lake water, bacterial mats and sediments within the lake (Table 2). Only leaves were used for the bulk and lipid analyses of the modern plant material (identification T. C. Partridge and C. Löser, pers. commun.). We recovered 14 samples from 2 to 7 m depth in a composite core taken in November 2001 to February 2002. The core samples average over 5–10-cm intervals to assure similar time coverage for all (~150 years). With exception of the water samples, all samples were freeze-dried, ground and homogenised before extraction. The water samples were extracted using the method of Bligh and Dyer (1959). Sediment and plant samples were extracted by accelerated solvent extraction or flow blending (Radke et al. 1978) using a mixture of dichloromethane and methanol (99/1, v/v) as a solvent. The extracts were separated by medium-pressure liquid chromatography (Radke et al. 1980) into fractions of aliphatic/alicyclic hydrocarbons, aromatic hydrocarbons and nitrogen, sulphur and oxygen (NSO) compounds. Further separation of the NSO compounds into a neutral NSO compound and a more polar fatty acid fraction was achieved following a modified method of McCarthy and Duthie (1962). Trimethylsilylation of the neutral NSO compound fraction was carried out using MSTFA (*N*-Methyl-*N*-(trimethylsilyl)trifluoroacetamide).

Gas chromatography (GC-FID), gas chromatography–mass spectrometry (GC–MS) and isotope ratio monitoring–gas chromatography–mass spectrometry (IRM–GC–MS)

Identification and quantification of individual compounds within the aliphatic hydrocarbon and the neutral NSO compound fraction was achieved using GC and GC–MS techniques. GC analysis was performed on an Agilent 6890 Series instrument equipped with a cold injection system and an Ultra 1 methyl siloxane fused silica capillary column [50 m length, 0.2 mm inner diameter (ID), 0.33 µm film thickness (FT)]. Helium was used as carrier gas, and the temperature of the GC oven was programmed to an initial temperature of 40°C (hold 2 min), a heating rate of 5°C min⁻¹, and a final temperature of 300°C, held isothermal for 65 min. The injector temperature rose from initially 40 to 300°C (hold 3 min) at a rate of 700°C min⁻¹. The MS-coupled GC Thermo GC

Ultra was equipped with a Thermo PTV injection system and a SGE BPX5 fused silica capillary column (50 m length, 0.22 mm ID, 0.25 µm FT). Helium was used as carrier gas, and the temperature of the GC oven was programmed from 50°C (hold 1 min) to 310 or 350°C at a rate of 3°C min⁻¹, followed by an isothermal phase of 30 min. The injector temperature was programmed from 50 to 300°C at a rate of 10°C s⁻¹. A DSQ Thermo Finnigan Quadrupole MS, operating in the electron impact ionisation mode (EI) at 70 eV, was used for compound identification. Full scan mass spectra were recorded from *m/z* 50 to 600 (hydrocarbons) or 650 (neutral NSO compounds) at a scan rate of 2.5 scans s⁻¹. Compound identifications are based on comparison of mass spectra to those reported in the literature, in the NIST mass spectral database, and on comparison with authentic standards.

The carbon isotopic composition of saturated hydrocarbons was measured using IRM–GC–MS. The IRM–GC–MS system consisted of a GC unit (6890N, Agilent Technology, USA) connected to a GC III combustion device coupled via open split to a MAT 253 mass spectrometer (ThermoFisher Scientific, Germany). Three microliter of the aliphatic hydrocarbon fraction were injected to the programmable temperature vaporisation inlet (PTV, Agilent Technology, USA) with a septumless head, working in split/splitless mode. The injector was held at a split ratio of 1:1 and an initial temperature of 230°C. With injection, the injector was heated to 300°C at a programmed rate of 700°C min⁻¹ and held at this temperature for the rest of the analysis time. The aliphatic hydrocarbon fractions were separated on a fused silica capillary column (HP Ultra 1, 50 m length, 0.2 mm ID, 0.33 µm FT, Agilent Technology, Germany). The temperature program started at 40°C and was then increased to 300°C at a rate of 3°C min⁻¹, held there for 25 min. Helium, set to a flow rate of 1.0 ml min⁻¹, was used as carrier gas. The organic compounds in the GC effluent stream were oxidised to CO₂ in the combustion furnace held at 940°C on a CuO/Ni/Pt catalyst. CO₂ was transferred on line to the mass spectrometer to determine carbon isotope ratios. All samples were measured in triplicate with a standard deviation of ≤0.5‰ for most of the compounds and samples. The isotopic ratios including δ¹³C_{org} are given in delta notation relative to Vienna PeeDee Belemnite (VPDB).

$$\delta_{\text{sample}}(\text{‰}) = \left[\left(\frac{(^{13}\text{C}/^{12}\text{C})_{\text{sample}}}{(^{13}\text{C}/^{12}\text{C})_{\text{standard}}} - 1 \right) \times 1000 \right]$$

Analysis of total organic carbon content (TOC) and stable carbon isotope ratios of bulk organic matter ($\delta^{13}\text{C}_{\text{org}}$)

Determinations of the TOC and $\delta^{13}\text{C}_{\text{org}}$ of the sediment were carried out on decalcified samples. Approximately 3 mg of sediment were weighed in Ag capsules, treated with 20% HCl, heated for 3 h at 75°C, and finally wrapped up in the Ag capsules. For the plant material analyses, about 2 mg of dried and homogenized material was wrapped up in tin capsules. The carbon content and $\delta^{13}\text{C}$ values were measured using a CarloErba NC2500 elemental analyzer coupled via a ConFlowIII interface with a DELTAplusXL mass spectrometer (ThermoFisher Scientific, Bremen). The samples were combusted under excess oxygen and the released gases were flushed by a helium carrier-gas flow into the IRMS. The isotopic ratios are given in delta notation relative to VPDB. The calibration was performed using isotopic standards (USGS24, CH-7) and proven with a soil reference sample (Boden2). The precision for replicate analyses is 0.2% for TOC and better than 0.2‰ for $\delta^{13}\text{C}$.

Chronology

The age model of the profile is based on nine radiocarbon ages determined by the Poznań Radiocarbon Laboratory (Table 1). Three of the radiocarbon ages are obtained from microscopic charcoal fragments, and the others from bulk OM. The ages show a regular increase with depth. For details on the litho- and chronostratigraphy we refer to Kristen et al. (2007).

Results

Biomarker composition of the present-day environment and sediments

We sampled floating cyanobacterial mats which dominate the present-day aquatic ecosystem of the Tswaing Crater (Ashton 1999) and are identified as *Oscillatoria* sp. by marker-pigments oscillaxanthin, myxoxanthophyll and echinenon (S. Fietz, pers. commun.). The aliphatic hydrocarbon fraction of *Oscillatoria* sp. consists predominantly of the C_{17} *n*-alkane with minor contributions of C_{15} and C_{16} *n*-alkanes and C_{17} *n*-alkenes (Fig. 2a; Table 2). In the neutral NSO compound fraction of these floating cyanobacterial mats, phytol (II; roman numerals refer to structures of biomarkers given in ESM1) is the overall dominant compound (Table 2). In the very

Table 1 Radiocarbon ages for the Lake Tswaing sediment core from 2001/2002

Original depth (m)	Corrected depth (m)	Lab no.	^{14}C age (years BP)	SD±	Calibrated age (years BP)	$\pm 2\sigma$	Material
1.595–1.605	0	Poz-15663	3,095	35	1,810* ^a	91	TOC
2.21–2.24	0.61–0.64	Poz-15669	3,675	35	2,538* ^a	175	TOC
4.005–4.065	2.405–2.465	Poz-12211	4,305	30	4,837*	35	Charcoal
5.23–5.24	3.63–3.64	Poz-15664	7,090	50	7,850*	115	TOC
7.36–7.38	5.54–5.56	Poz-15665	13,130	70	15,550*	356	TOC
9.785–9.795	7.695–7.705	Poz-15667	20,410	130	24,440*	405	TOC
11.835–11.885	9.705–9.755	Poz-12212	28,500	600	33,220**	1,072	Charcoal
16.990–17.020	14.790–14.820	Poz-12213	31,900	800	37,390**	1,120	Charcoal
19.385–19.395	17.195–17.205	Poz-15668	44,800	2,100	48,440**	2,559	TOC

* Calib 5.0.2 after McCormac et al. (2004) and Reimer et al. (2004)

** CalPal (calibration curve CalPal2005_SFCP; <http://www.calpal.de>)

^a Including 1,150 years reservoir correction (mean age offset of recent lake sediments; Partridge et al. 1997)

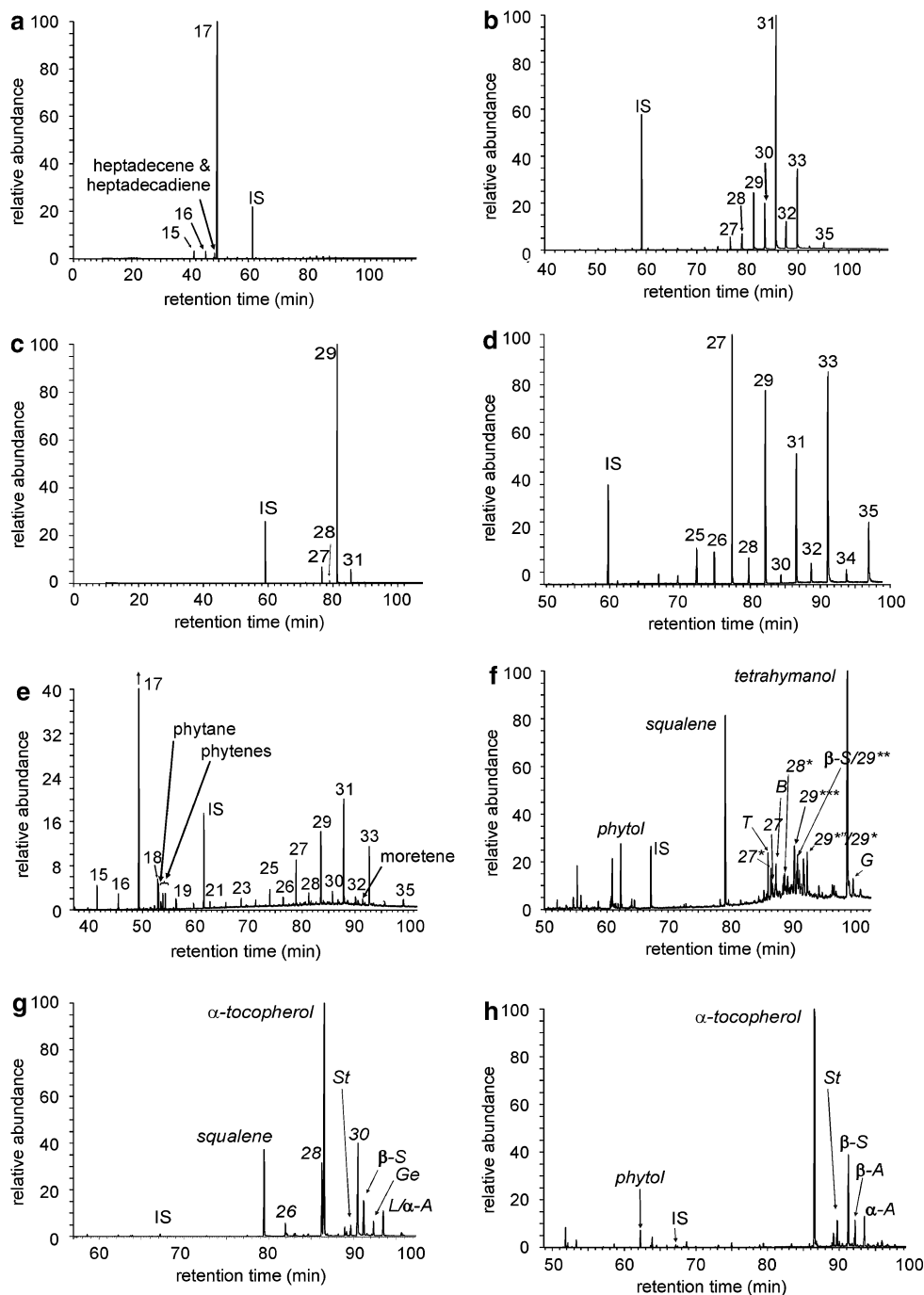


Fig. 2 TIC chromatograms of modern plant and sediment samples from the Tswaing Crater (IS = internal standard, for other labels see Table 2); **a** aliphatic hydrocarbon fraction of planktonic cyanobacteria (*Oscillatoria* sp.); **b** aliphatic hydrocarbon fraction of *Typha angustifolia*; **c** aliphatic hydrocarbon

fraction of *Acacia tortilis*; **d** aliphatic hydrocarbon fraction of unknown grass; **e** aliphatic hydrocarbon fraction of modern lake sediment; **f** neutral NSO compound fraction of microbial mat sample; **g** neutral NSO compound fraction of *Acacia karoo*; **h** neutral NSO compound fraction of *Typha angustifolia*

Table 2 Concentrations of abundant biomarkers identified in modern samples from the Tswaing Crater

Compounds	Abbr. (Fig. 2)	Structure in App.	Sample no. ^a (concentrations in $\mu\text{g/g}$ TOC if not quoted otherwise)														
			1	2	3 ^b	4 ^b	5	6	7	8	9	10	11	12	13	14	
C ₁₅ <i>n</i> -alkane	15		9	ND	ND	1.1											62
C ₁₆ <i>n</i> -alkane	16		46	ND	ND	1.0											19
C ₁₇ <i>n</i> -alkane			141	ND	ND	0.26											5
C ₁₇ <i>n</i> -alkane	17		1,741	ND	ND	20											652
C ₁₈ <i>n</i> -alkane	18		24	ND	ND	0.9											48
C ₁₉ <i>n</i> -alkane	19		4	ND	ND	0.35											
C ₂₅ <i>n</i> -alkane	25		6	ND	ND	0.23	65	8	26		11	11	9	7	58		
C ₂₇ <i>n</i> -alkane	27		9	ND	ND	0.26	447	25	212	70	25	20	41	7	371		
C ₂₉ <i>n</i> -alkane	29		14	ND	ND	0.26	1,300	85	1,666	23	58	50	157	12	282		
C ₃₁ <i>n</i> -alkane	31		14	ND	ND	0.27	693	64	178		30	287	497		204		
C ₃₃ <i>n</i> -alkane	33		7	ND	ND		270	16			168	267			439		
C ₃₅ <i>n</i> -alkane	35			ND	ND										200		
1-Octadecanol			18														32
1-Icosanol														71	ND		
1-Hexacosanol	26							232			147	71			ND		
1-Octacosanol	28		5		49	0.11	1,236	1,770	9	1,527	418			221	ND		
1-Triacontanol	30		3	3	0.10		3,071	15	2,365	731				3,014	ND		
3,7,11,15-Tetramethyl-hexadecenol (phytol)		II	261	28	1.3	1.9	144	53					184	45	ND	1,680	
Squalene		I	38	87	70	4	92	175		3,264	522	1,208		65	ND		
α -Tocopherol	<i>T</i>	III	13	23	9	1.2	497	2,735		625	1,802	850	3,787	578	ND		
Cholest-5-en-3 β -ol	27*	Va	18	20		0.53									ND		
5 α (H)-cholestan-3 β -ol	27	IV	5			0.10									ND		
24-Methyl-cholesta-5,22-dienol (brassicasterol)	<i>B</i>	IXa	15			0.35									ND		
C29 cholestanol			7			0.24									ND		
24-Methylcholest-5-en-3 β -ol	28*	Vb	11			0.33		235						496	ND		
24-Ethylcholesta-5,22-dien-3 β -ol (stigmasterol)	<i>Sr</i>	IXb	14	8		0.42		479		273	76	52	428	1,875	ND		
24-Ethyl-cholesta-5,7,22-trien-3 β -ol	29***	VIII	53			3									ND		
24-Ethylcholest-5-en-3 β -ol (β -sitosterol)	β -S	Vc	13	12		0.54	414	1,779		420	288	244	1,600	2,015	ND		
24-Ethylcholesta-7,22-dien-3 β -ol	29**	VII	28			0.48									ND		
4,24-Dimethyl-cholest-5-en-3 β -ol/24-ethyl	29*	XI													ND		
-Cholest-7-en-3 β -ol	29*	VI	32			1.2									ND		

Table 2 continued

Compounds	Abbr. (Fig. 2)	Structure in App.	Sample no. ^a (concentrations in µg/g TOC if not quoted otherwise)													
			1	2	3 ^b	4 ^b	5	6	7	8	9	10	11	12	13	14
Olean-18-en-3β-ol (germanicol)	Ge	XV								115						ND
Olean-12-en-3β-ol (β-amyrin)	β-A	XIV			6									450		ND
Urs-12-en-3β-ol (α-amyrin)/	α-A	XII														
Lup-20(29)-en-3β-ol (lupeol)	L	XVI			46					232				543		ND
Tetrahymanol		Xb		46	224						12					ND
Gammaceran-3-one	G	Xa									0.64					55

^a 1, Bacterial mat (solid); 2, bacterial mat (fluid); 3, water (surface); 4, water (~30 cm), 5, *Sclerocarya* ("caffra") *birrea*; 6, *Acacia robusta*; 7, *Acacia tortilis*; 8, *Zizyphus mucronata*; 9, *Acacia karoo*; 10, *Combretum apiculatum*; 11, *Typha angustifolia*; 12, Cyperaceae; 13, grass (*Digitaria* sp.); 14, floating cyanobacteria (*Oscillatoria* sp.)

^b Concentration in µg/mg extractable lipids

ND not determined

shallow lake areas, benthic microbial mats reveal an aliphatic hydrocarbon fraction that is dominated by C₁₇ *n*-alkane and -alkene similar to the floating cyanobacterial mats. In the neutral NSO compound fraction, the benthic microbial mats differ clearly from the floating cyanobacterial matter. Tetrahymanol (Xb), squalene (I), and phytol dominate a complex mixture of saturated and unsaturated steroidal alcohols with 27–29 carbon atoms (Fig. 2f). Tetrahymanol, squalene and phytol also prevail in extracts of water samples from Lake Tswaing from ~30 cm water depth (Table 2).

Macrophytes along the lake shore comprise predominantly *Typha angustifolia* and *Cyperacea* sp. *Typha angustifolia* exhibits a clear odd-numbered carbon preference of the *n*-alkanes maximising at *n*-C₃₁ (Fig. 2b; Table 2), whereas *Cyperacea* sp. contains low amounts of *n*-alkanes with maxima at *n*-C₂₃ and *n*-C₂₉ (Table 2). The surrounding higher land plant assemblage along the crater wall is dominated by grasses and different species of *Acacia*, *Combretum*, *Sclerocarya* and *Zizyphus* (Fig. 1). The aliphatic fraction of leaf tissue from these plants contains predominantly C₂₇ to C₃₃ long-chain *n*-alkanes with a strong odd-numbered carbon preference (Fig. 2a–d; Table 2). The individual land plant species show differing distribution patterns of *n*-alkanes with *Acacia tortilis* (Fig. 2c), *Acacia karoo*, *Acacia robusta* and *Sclerocarya birrea* maximising at *n*-C₂₉, *Combretum apiculatum* maximising at *n*-C₃₁, *Zizyphus mucronata* maximising at *n*-C₂₇ and grasses exhibiting two maxima at *n*-C₂₇ and *n*-C₃₃. The neutral NSO compound fraction of *Typha angustifolia*, *Acacia robusta*, and *Acacia karoo* is dominated by α-tocopherol (vitamin E) (III). It is present as a major constituent in most of the investigated modern plant and water samples (Fig. 2f–h). Stigmasterol (24-ethylcholesta-5,22-dien-3β-ol) (IXb), β-sitosterol (24-ethylcholest-5-en-3β-ol) (Vc), β-amyrin (olean-12-en-3β-ol) (XIV), α-amyrin (urs-12-en-3β-ol) (XII), lupeol (lup-20(29)-en-3β-ol) (XVI) and germanicol (olean-18-en-3β-ol) (XV) are characteristic triterpenoidal alcohols in the investigated higher land plants and macrophytes (Fig. 2g, h; Table 2). Phytol and squalene, major compounds in the autochthonous lake organisms, are also present in the investigated higher land plants and macrophytes. In *Zizyphus mucronata* and *Combretum apiculatum*, squalene is the dominant compound. The C₂₈ and C₃₀ *n*-alkanols

are the only straight-chain alcohols that are abundant in the modern leaf material (Table 2).

The aliphatic fraction of the extractable OM of modern Lake Tswaing sediments predominantly consists of odd-numbered *n*-alkanes and reveals a bimodal distribution maximising at *n*-C₁₇ and *n*-C₃₁ (Fig. 2). Phytane, phytene and moretene (XIII), identified as additional compounds in the sediments, have not been detected in any of the investigated modern organisms or water samples from the Tswaing Crater. The composition of the neutral NSO compounds of the sediments resembles the one of water and mat samples, except that tetrahymanol is the overall dominant compound; squalene has not been detected in the sediments and phytol and α -tocopherol contents are minor.

Stable carbon isotope composition of organic constituents of the modern ecosystem

For bulk floating cyanobacterial matter we observe a $\delta^{13}\text{C}_{\text{org}}$ of -24.0‰ . The C₁₇ *n*-alkane of floating cyanobacteria is 10.6‰ depleted in ¹³C relative to the bulk material (ESM Table 1). Microbial mats in the shallow lake area are characterised by a relatively high $\delta^{13}\text{C}_{\text{org}}$ value of -18‰ . The investigated trees and bushes listed in Table 2, except the grasses and macrophytes, show $\delta^{13}\text{C}_{\text{org}}$ values between -25.5

and -30.7‰ . The dominant long-chain *n*-alkanes (*n*-C_{27,29,31,33}) have $\delta^{13}\text{C}$ values of -26.9 to -37.6‰ . The investigated macrophytes *Typha angustifolia* and *Cyperaceae* sp., and the grasses show $\delta^{13}\text{C}_{\text{org}}$ values of -11.4 to -13.2‰ . The dominant *n*-alkanes *n*-C₂₃ and *n*-C₂₉ of *Cyperaceae* sp. range from -24.9 to -27.2‰ , and the dominant *n*-alkanes *n*-C₂₇ and *n*-C₃₃ of *Typha angustifolia* range from -20.1 to -22.6‰ , resulting in a fractionation of 10–15‰ compared to the bulk plant material.

Modern sediments from Lake Tswaing are characterised by a $\delta^{13}\text{C}_{\text{org}}$ signature of -16.8 to -17.7‰ (Fig. 3). Long-chain *n*-alkane $\delta^{13}\text{C}$ values (*n*-C_{27,29,31,33}) are intermediate between those of C3 plants and macrophytes and range from -21.5 to -27.9‰ . The isotopic composition of mid-chain *n*-alkanes corresponds to values found in modern macrophytes. Only the $\delta^{13}\text{C}$ of *n*-C₁₇ is higher in the sediments (-26‰) than in the sampled floating cyanobacteria (-34.6‰). The isotopic composition of moretene is more than 10‰ lower than the values of any other compound in the sediments.

Occurrence of long-chain alkenones in core sediments

Long-chain di-, tri-, and tetra-unsaturated alkenones (LCAs) with chain lengths ranging from C₃₇ to C₃₈

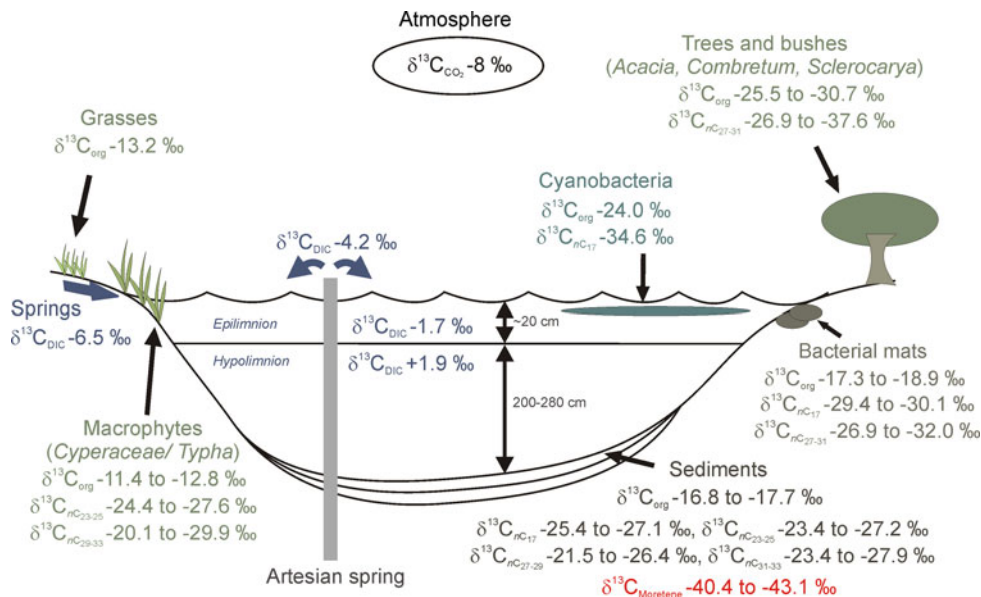


Fig. 3 Sketch with main components of the modern ecosystem and their relative stable carbon isotopic composition of bulk tissue and selected biomarkers from the aliphatic hydrocarbon fraction

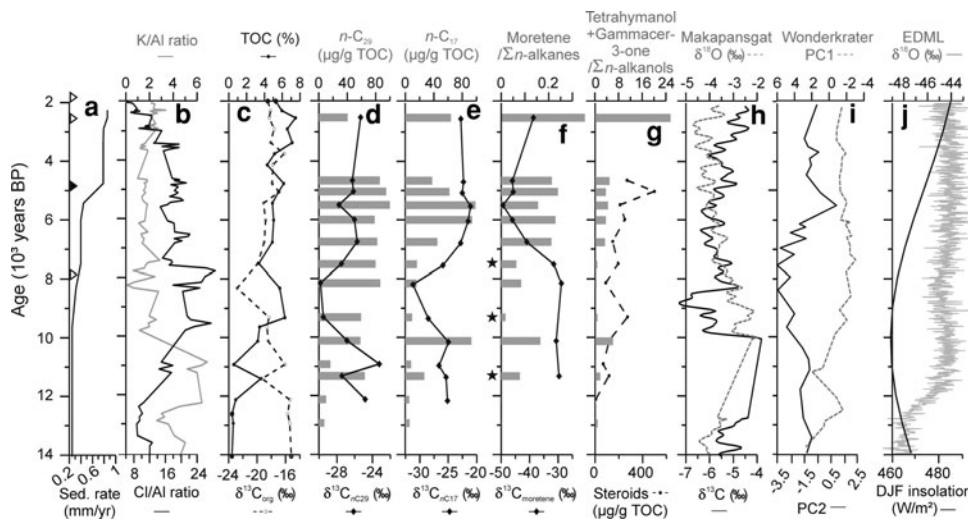


Fig. 4 Downcore plots of **a** sedimentation rate, based on radiocarbon ages from Table 1; **b** K/Al (grey) and Cl/Al (black) intensity ratios from XRF-core scanning (modified after Kristen et al. 2007); **c** $\delta^{13}\text{C}_{\text{org}}$ (dashed line) and total organic carbon content (TOC, black line); **d–f** $\delta^{13}\text{C}$ of selected aliphatic biomarkers (black lines), in comparison with the concentration of the respective biomarkers or the ratio of moretene versus *n*-alkanes (**f**, grey bars, stars highlight the samples which contain long-chain alkenones); **g** ratio of tetrahymanol + gammaceran-3-one (diagenetic product of tetrahymanol) versus *n*-alkanols (grey bars) and concentration

of terrestrial steroids (dashed line) of Lake Tswaing sediments; in comparison with **h** $\delta^{13}\text{C}$ (black line) and $\delta^{18}\text{O}$ (dashed line) from a stalagmite from Makapansgat Valley (24°8.824'S, 29°10.371'E) (Holmgren et al. 2003); **i** the temperature (PC1, dashed line) and humidity indices (PC2, black line) derived from the Wonderkrater pollen record (24°25.806'S, 28°44.626'E) (Scott and Holmgren 2003); **j** $\delta^{18}\text{O}$ record from Antarctic ice core from Dronning Maud Land (EDML) (Members 2006, grey) and changing summer (mean December, January and February, DJF) insolation at 30°S

are detected in three samples from the early to mid Holocene (marked with stars in Fig. 4). In contrast to previous studies (Li et al. 1996; Thiel et al. 1997; Zink et al. 2001), we do not observe a decrease in concentration with increasing chain length of LCAs. Furthermore, the tetra-unsaturated compounds are very low in concentration compared to the tri-unsaturated ketones (Fig. 5).

Discussion

Biomarker sources

The dominance of cyanobacteria in the modern lacustrine environment of the Tswaing Crater as well as their biomarker inventory with the prominent C_{17} *n*-alkane are typical for saline and alkaline lakes (Grimalt et al. 1991; Rontani and Volkman 2005). Phytol, the most abundant compound of the cyanobacterial NSO compound fraction, is an ubiquitous compound in samples from the Tswaing Crater and in aquatic environments in general as it arises in most

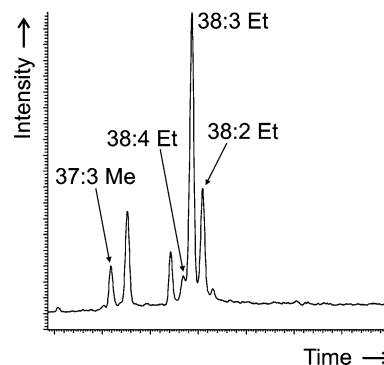


Fig. 5 Gas chromatogram showing the long-chain alkenone (di-, tri- and tetra-unsaturated methyl and ethyl ketones) distribution in a sediment sample from Lake Tswaing (3.5 m depth, 7,500 years BP)

cases from the degradation of chlorophylls (Rontani and Volkman 2003). It can therefore result from autochthonous and allochthonous OM. The virtual absence of sterols in the sample from floating cyanobacteria agrees with the conclusion of Volkman (2005) that these organisms are not able to produce sterols. The biomarker composition of benthic

microbial mats and of deeper lake waters are much more complex. Most abundant are unsaturated C₂₉ steroid compounds (Fig. 2f; Table 2) which are known from cyanobacterial mats as well as from other microorganisms such as marine phytoplankton (Boon et al. 1983). They have also been reported from other saline lakes (Grimalt et al. 1991; Pearson et al. 2007). Tetrahymanol has been frequently identified in marine ciliates (Harvey and McManus 1991), but was also found in lake waters (Grimalt et al. 1991; Pearson et al. 2007; Thiel et al. 1997), in coastal bacterial mats (Rontani and Volkman 2005), and in the phototrophic bacterium *Rhodopseudomonas palustris* (Kleemann et al. 1990). As Harvey and McManus (1991) documented that tetrahymanol is only produced by ciliates when dietary sterol supply is poor or absent, we attribute the presence of tetrahymanol to the activity of the photosynthetic sulphur bacterium *Rhodopseudomonas palustris*, since sterols are abundant in Lake Tswaing. This organism is known to be common in water and soils, and to be metabolically versatile; it is able to thrive in the absence or presence of oxygen and to fix nitrogen (Larimer et al. 2003)—abilities, that possibly favour its growth in Lake Tswaing under the prevailing aquatic conditions. Oxidation of tetrahymanol results in gammaceran-3-one (Xa) (Thiel et al. 1997), which is present in small amounts in the samples from deeper lake waters and commonly occurs in the sediments. However, oxidation can not be too severe since tetrahymanol is a prominent compound in the sediments of the core down to 40 m depth (ca. 100 k years BP) (Kristen, unpublished data) whereas phytol, α -tocopherol and squalene are degraded and lost from the sediments. Squalene, which is abundant in all samples of the modern crater environment, is the biosynthetic precursor of steroids in higher organisms and of hopanoids in bacteria (Volkman 2005). Boon et al. (1983) observed squalene in cyanobacterial mats from a solar lake, but it is also reported as a major component in halophilic archaea and methanogens (Tornabene et al. 1979). We consider it being of predominantly bacterial origin in Lake Tswaing, although neither a contribution of halophilic archaea, nor a contamination of the mat by surrounding higher plants, in which squalene is also present, can be ruled out. Most likely, a multitude of microorganisms contribute to the observed signal in the samples from benthic microbial mats and deeper

waters, and also input from land plants is likely to occur as indicated by the presence of β -sitosterol.

The *n*-alkane distribution observed in higher land plants and macrophytes of the Tswaing Crater is in agreement with earlier observations (Eglinton and Hamilton 1963). The most abundant sterol compounds (Table 2) have been described as typical constituents of vascular plants and in other studies on lacustrine systems (Pearson et al. 2007; Volkman 2005). The prominent occurrence of α -tocopherol in the NSO compound fraction has also been reported for higher land plants, cyanobacteria, and micro- and macroalgae (Rontani and Volkman 2005).

The composition of the extractable OM of modern Lake Tswaing sediments corresponds to a mixture of individual sources that include lake organisms, macrophytes, and higher land plants. The additionally occurring phytane and phytanes in the sediments have been described from other alkaline (Grimalt et al. 1991) and hypersaline (Boon et al. 1983) environments. Phytane and phytanes are often interpreted as products of phytol from the side-chain of chlorophyll-*a* which form during early diagenesis in anoxic environments (Tissot and Welte 1984). The frequent occurrence of phytol in modern organisms from the Tswaing Crater together with the prevailing anoxic conditions in the deeper water column would support such an interpretation. However, this pathway has not been proved so far (Grossi et al. 1996; Rontani and Volkman 2003). In methanogenic archaea, phytane and phytanes are unambiguously detected (Tornabene et al. 1979). Additionally, the formation of phytanes and phytadienes has been reported from anaerobic biodegradation of phytol by sulphate-reducing bacteria (Grossi et al. 1998). Both processes can contribute to the phytanes observed in modern anoxic sediments from Lake Tswaing. Sulphate reduction as a prominent process in Lake Tswaing was already proposed by Ashton (1999) who measured a strong gradient in sulphate concentration from 300 mg l⁻¹ in 25 cm water depth to 0.5 mg l⁻¹ in 1 m water depth. The strong odour of H₂S from water samples below 0.5 m water depth supports this interpretation. The hopanoid biomarker moretene (17 β (H)-moret-22(29)-ene or isohop-22(29)-ene), which occurs in the sediments from Lake Tswaing, has been rarely reported in the literature. It was found in sediments especially from acidic lakes in Japan and from Lake Baikal (Uemura and Ishiwatari 1995), in early Holocene (limnic)

sediments from the Black Sea (Blumenberg et al. 2009) and possibly also in sediments from an alkaline lagoon in Spain (Grimalt et al. 1991). We follow indications of Blumenberg et al. (2009) and Uemura and Ishiwatari (1995) and attribute the occurrence of moretene in the sediments of Lake Tswaing to the activity of methanotrophic bacteria. Consequently, a derivation of moretene, phytane and phytanes from a microbial community including methanotrophic and sulphate-reducing bacteria, and maybe also methanogenic archaea, which thrives in the deeper water column or at the sediment/water interface, is inferred.

Three samples from the Lake Tswaing sediment core (marked with stars in Fig. 4) contain LCAs with chain lengths ranging from C₃₇ to C₃₈. These samples have an age of 11,500–7,500 years BP, TOC concentrations above 0.5% but low concentrations of tetrahymanol and moretene (Fig. 4), and relatively high $\delta^{13}\text{C}$ values for moretene. Likewise, Thiel et al. (1997) found high amounts of LCAs in samples with low concentrations of tetrahymanol/gammaceran-3-one in a sediment sequence from the highly alkaline Lake Van in Turkey. They attribute higher concentrations of LCAs to periods of increased convection and nutrient availability but source organisms remained unknown. LCAs are increasingly found in lacustrine environments at high and low latitudes (Li et al. 1996; Pearson et al. 2007; Thiel et al. 1997; Zink et al. 2001). Identified source organisms for LCAs are predominantly members of Prymnesiophyceae, but other groups are discussed (Zink et al. 2001). In *Chrysothila lamellosa*, a non-calcifying haptophyte that was shown to be an important alkenone producer especially in brackish water, C₃₇ alkenones dominate over C₃₈ alkenones and concentrations of tetra-unsaturated LCAs decrease with increasing growth temperatures in the investigated range from 10 to 22°C (Sun et al. 2007). Assuming water temperatures at the higher end of this calibration range in Lake Tswaing before 7,500 years BP (for comparison, lowest seasonal lake water temperature observed today is 19.7°C, Ashton 1999), low concentrations of tetra-unsaturated LCAs in Lake Tswaing sediments are in agreement with the observation of Sun et al. (2007). However, in Lake Tswaing sediments C₃₈ dominate over C₃₇ alkenones (Fig. 5). The same appears to be the case for lakes in semi-arid regions of Spain, where Pearson et al. (2007) found LCAs dominated by tri-unsaturated C₃₈

alkenones. A similar or even identical but yet unidentified producer of LCAs in these ecosystems is very likely, especially when considering that both the South African and the Spanish sites are warm and shallow lakes and predominantly hypersaline and alkaline environments. In contrast to Thiel et al. (1997), we do not think that nutrient availability plays an important role as LCAs in Lake Tswaing sediments occur in samples from the presumably more arid period 10,000–7,500 years BP, when lake productivity was diminished due to nutrient scarcity, and also in one sample from ca. 11,300 years BP, when nutrient availability allowed higher lake productivity. We tentatively conclude that the presence/absence of LCAs in sediments from Lake Tswaing depends on changes within the microbial community of the lake. As indicated by the $\delta^{13}\text{C}$ signature of moretene, methanotrophic organisms established after ca. 7,500 years BP when LCA producing organisms disappeared.

The carbon cycle of the Tswaing Crater: stable carbon isotope ratios of organic constituents of the modern ecosystem

The $\delta^{13}\text{C}_{\text{org}}$ of -24.0‰ for bulk floating cyanobacterial matter from Lake Tswaing is consistent with a ^{13}C -depletion of $\sim 22\text{‰}$ relative to the carbon source observed by Sakata et al. (1997) in laboratory experiments and a $\delta^{13}\text{C}_{\text{DIC}}$ of -1.7‰ of the modern surface waters. This $\delta^{13}\text{C}_{\text{DIC}}$ reflects the predominance of bicarbonate and carbonate in the water under a prevalent pH of 9–10. The isotopic signature of the C₁₇ *n*-alkane from floating cyanobacteria is 10.6‰ lower relative to the bulk material. This difference is for unknown reasons slightly larger compared to earlier investigations from Sakata et al. (1997) with -8.4‰ . The relatively high $\delta^{13}\text{C}_{\text{org}}$ value of -18‰ from microbial mats in the shallow lake area is comparable to published data from hypersaline microbial mats (Schouten et al. 2001).

In accordance with literature, the $\delta^{13}\text{C}_{\text{org}}$ values of investigated trees and bushes (-25.5 to -30.7‰) and of the grasses (-13.2‰) fall within the range commonly associated with C3 plants and C4 plants, respectively (O'Leary 1981). The 1.4–6.9‰ lower signature of the dominant long-chain *n*-alkanes (*n*-C_{27,29,31,33}) of trees and bushes further corresponds to results Collister et al. (1994) reported for *n*-alkanes

of C3 plants with 1.6–8.9‰ ^{13}C -depletion. The investigated macrophytes *Typha angustifolia* and *Cyperaceae* sp., however, show $\delta^{13}\text{C}_{\text{org}}$ values and a fractionation between dominant *n*-alkanes and bulk plant material as it is typically attributed to C4 plants (Collister et al. 1994). Whereas the family *Cyperaceae* includes both C3 and C4 plant species, *Typha* sp. is jointly classified as C3 plant and $\delta^{13}\text{C}_{\text{org}}$ values of *Typha* leaves have been described in the range of –26.4 to –29.4‰ (Hornibrook et al. 2000; Wang et al. 2003). Street-Perrott et al. (2004) stated that macrophytes are able to use HCO_3^- as carbon source which would lead to higher $\delta^{13}\text{C}$ values. Additionally, conditions of a dry or saline habitat can cause a shift in the $\delta^{13}\text{C}$ signature of plants to higher values (Wooller et al. 2007). The unusually high $\delta^{13}\text{C}$ value as well as the increased fractionation between bulk plant material and *n*-alkanes of *Typha angustifolia* from the Tswaing Crater is interpreted to result from a combination of these two effects.

The $\delta^{13}\text{C}$ values of modern sediments from Lake Tswaing are widely reflecting the mixed input of OM from autochthonous and allochthonous sources. This mixture is indicated by $\delta^{13}\text{C}_{\text{org}}$ as well as compound-specific $\delta^{13}\text{C}$ signals of the sediment samples. Long-chain *n*-alkane $\delta^{13}\text{C}$ values (*n*-C_{27,29,31,33}) are intermediate between those of C3 plants and macrophytes (Fig. 3). The isotopic composition of mid-chain *n*-alkanes corresponds to values found in modern macrophytes. The 7.5–9.2‰ higher $\delta^{13}\text{C}$ of *n*-C₁₇ in the sediments compared to the $\delta^{13}\text{C}$ of *n*-C₁₇ of sampled floating cyanobacteria is interpreted to be associated with seasonal or inter-annual differences in the $\delta^{13}\text{C}$ signature of the water column and corresponding cyanobacterial blooms, which are integrated in the top few centimeters of sediment. Alternatively, it is also possible that microbial mats from the lake shore contribute to this signal. Moretene, which is only found in the sediments, is characterised by more than 10‰ lower $\delta^{13}\text{C}$ values compared to other compounds in the sediments. This is interpreted as a contribution of moretene from bacteria or a bacterial community living in the deeper water column of Lake Tswaing or at the sediment surface and feeding on a carbon source isotopically depleted in ^{13}C . This carbon source might be a mixture of degraded OM from the photic zone and oxidised methane, or methane directly consumed by methanotrophs as suggested by Blumenberg et al.

(2009) and Uemura and Ishiwatari (1995). In this context, the detection of an unusually high $\delta^{13}\text{C}_{\text{DIC}}$ signature at 50 cm water depth (+1.9‰) might confirm that methane generation occurs in Lake Tswaing (Rosenfeld and Silverman 1959) (Fig. 3).

Tracing the changing carbon cycle in the Tswaing Crater: a sediment core study (ca. 14,000–2,000 years BP)

For the palaeoenvironmental study, we infer changes in the lacustrine, near-surface primary productivity, which is probably predominantly cyanobacterial, from changes in the concentration of the C₁₇ *n*-alkane. Changes in the concentration and carbon isotopic composition of moretene are thought to reflect bacterial activity in the bottom water or at the sediment/water interface. The concentration of tetrahymanol additionally indicates the varying contribution of bacterial biomass in the lake. Changes in the stable carbon isotope composition of the C₂₉ *n*-alkane are most probably related to changes in the relative contribution of bushes and trees (C3 plants) versus grasses and macrophytes (C4-type signal). Variable amounts of the sterols which were identified in the modern higher plants further trace changes in the abundance of higher plants around the lake.

The total amount of biomarkers, as TOC content in general, is very low in samples from 14,000–10,000 years BP with the exception of a short period around 11,300 years BP (Fig. 4). This indicates that productivity in and around the lake was reduced due to unfavourable climatic conditions and/or that hydrology did not allow preservation of OM during this time. In a preceding study (Kristen et al. 2007), we compared XRF data from the current profile to mineralogical data from a previously studied core from Lake Tswaing (Bühmann and Elsenbroek 1999). We interpreted the correspondence of high relative proportions of detrital minerals (quartz, mikrokline, plagioclase) with high potassium, aluminium, and iron intensities in combination with low chlorine intensities and TOC contents as indication for increased sheet wash and reduced lake water salinity and stability. These more humid conditions were observed for the period 15,000–10,000 years BP (Fig. 4b). Because sedimentation rates were relatively low during this time ($\sim 0.24 \text{ mm years}^{-1}$, Fig. 4a), reduced lake water salinity and increased

turbulence probably favoured microbial activity and OM degradation. Under these conditions, biomarker concentrations are too low to reliably determine compound-specific stable carbon isotope ratios. Results from a pollen and palaeomagnetic study from Lake Masoko (9°20.0'S, 33°45.3'E), however, support our interpretation. Both proxies indicate relatively humid conditions with a short dry season in the southern hemisphere tropics for the period 15,000–11,800 years BP (Garcin et al. 2007). Garcin et al. (2007) relate this observation to a probable southward position of the ITCZ. However, as this interval further coincides with observations of rising temperatures in the tropical Indian Ocean (Levi et al. 2007), the humid period may equally be connected to generally higher moisture availability in this region.

Around 11,300 years BP, probably only for a short period of a few hundred years, conditions became favourable for preservation of OM and biomarker concentrations increased (Fig. 4). This happened while K/Al ratios were elevated, indicating higher run-off from the catchment, and rising Cl/Al ratios point to enhanced evaporation, which was apparently strong enough to allow a stabilisation of the water column and OM preservation. We relate these observations to generally rising temperatures during Termination I, which are also reported from the Wonderkrater pollen sequence (Scott and Holmgren 2003) (Fig. 4i). The high variability of the Tswaing record in this time interval 12,500–10,000 years BP may be a reflection of the global climate oscillations during this period (Younger Dryas, Preboreal Oscillation) and/or relate to changes in the coupling of the tropical atmosphere and ocean circulation at the glacial/interglacial transition as suggested by Levi et al. (2007). Yet, reliably dated documentations of these phenomena are scarce in southern Africa, and resolution and uncertainties within the chronology of the sedimentary record presented here preclude more detailed interpretations. The increased OM content of this time slice allows compound-specific isotope analyses and reveals $\delta^{13}\text{C}$ values of *n*-C₁₇ similar to modern values (−25‰), indicating similar hydrological conditions in the past for photosynthetic organisms in the lake. The $\delta^{13}\text{C}$ value of *n*-C₂₉ of −27.5‰ is similar to the signal of modern C3 plants, but lower than the modern sedimentary signal (Fig. 3). This observation reflects a higher proportion of C3 plants in the surrounding of the lake and/or a lower

abundance of grasses and/or macrophytes. Pollen and stable carbon isotope studies from South Africa (Holmgren et al. 2003; Scott 2002) report, in contrast to studies from tropical Africa (Wooller et al. 2003), no expansion of C4 grasses under glacial conditions, making major changes in the C3/C4 proportion during Termination I unlikely. Therefore, the shift in $\delta^{13}\text{C}$ signatures probably results from a local decrease in input from grasses/macrophytes and/or less evaporative stress for macrophytes during a period with higher rainfall, as inferred from element distribution data (Kristen et al. 2007). Biomarkers typical for bacterial activity are also present around 11,300 years BP with $\delta^{13}\text{C}$ values of moretene approximately 10‰ more enriched in ¹³C than modern values. These data resemble values from terrestrial plant input and are only slightly lower than OM produced in the surface water. We therefore interpret the bacterial signal to result from bacteria degrading this OM.

With the beginning Holocene 10,500–10,000 years BP, all biomarker concentrations and especially the ones of autochthonously produced compounds rise significantly (Fig. 4). TOC contents of the sediments and the amounts of terrestrial biomarkers such as *n*-C₂₉ remain high from this time on or even show an increasing trend throughout the Holocene as does the contribution of terrestrial steroids. These observations point to continuously favourable conditions for higher plant vegetation in and around the crater, possibly in relation to the post-glacial warming, and continuously good preservation of organic matter in a more saline, stagnant lake (Kristen et al. 2007). Declining concentrations of *n*-C₁₇, moretene and tetrahymanol indicate strongly reduced lacustrine near-surface and bottom-lake productivity between 10,000 and 7,500 years BP. The contemporaneous decrease in the $\delta^{13}\text{C}$ signature of *n*-C₁₇ is consistent with reduced productivity in the lake surface waters (Leng et al. 2005). The $\delta^{13}\text{C}$ values of moretene, however, remain stable until ca. 7,500 years BP and imply no change in the bacterial community at the lake bottom during early Holocene times. In parallel, the $\delta^{13}\text{C}$ signal of *n*-C₂₉ decrease to around −30‰ which indicates a shift to a higher proportion of C3 vegetation around the lake and/or decreasing input from grasses/macrophytes and/or less evaporative stress for macrophytes. The time period 10,000–7,000 years BP, however, is recorded as the driest period of the last 20,000 years in the

Wonderkrater pollen record (Scott and Holmgren 2003). Elevated chlorine and low potassium intensities in the Tswaing sediments during this time interval further point to arid conditions at the site (Kristen et al. 2007) (Fig. 4b). The period 10,000–7,000 years BP coincides with times of dune formation in western Zambia (O'Connor and Thomas 1999), and with an exceptionally white interval in a stalagmite of the Makapansgat Valley that exhibits the lowest $\delta^{13}\text{C}$ values of the whole record (Holmgren et al. 2003) (Fig. 4h). The latter is interpreted as a period with reduced vegetation cover, especially reduced grass abundance. Combining the evidences from surrounding locations and from the Lake Tswaing record, the period 10,000–7,500 years BP appears to be a generally drier period, where the expansion of grasses and probably also macrophytes was reduced and the productivity of photosynthetic organisms in the lake was diminished. An orbitally induced northward shift of the ITCZ accompanied by a shortening of the rainy season (Garcin et al. 2007) can provide a possible mechanism, affecting particularly shallow rooting grasses. The consequential reduction in ground water inflow could have led to a shrinking of the lake area and the surrounding swamps as well as to reduced nutrient inflow into the lake, which in sum resulted in the observed decrease in primary productivity and $\delta^{13}\text{C}$ signals of the OM. The increased aridity for the southern subtropics appears to be linked to a northward expansion of the area influenced by the ITCZ according to observations from tropical and subtropical northern Africa (Ficken et al. 2002; Gasse 2000; Talbot and Lærdal 2000) where this interval represents a humid period.

After ca. 7,500 years BP, the amount of autochthonously produced OM increases again accompanied by a shift to higher $\delta^{13}\text{C}$ values of $n\text{-C}_{17}$, $n\text{-C}_{29}$ and TOC. These changes indicate a restart of near-surface lacustrine productivity and an increasing proportion of plants with a C4-type signal around the lake. It was probably caused by an increase of grasses and/or macrophytes around the lake and increased nutrient supply under more humid conditions. This trend continues until ca. 5,500 years BP and is complemented by the Wonderkrater pollen record that implies gradually more humid conditions maximising at ca. 5,500 years BP (Scott and Holmgren 2003) (Fig. 4i). Climate archives from northern subtropical and tropical Africa display increasing

aridity and/or stronger seasonality during the same period (Gasse 2000; Talbot and Lærdal 2000). This anti-phase behaviour of northern and southern hemisphere subtropics in response to precessional forcing has been frequently reported from climate archives of the African and American continents (Cruz et al. 2005; Fleitmann et al. 2003; Partridge et al. 1997). In parallel, the $\delta^{13}\text{C}$ signal of moretene decreases by 20‰ to a value of -50‰ at ca. 5,500 years BP. This value falls within a range typical for methane produced in freshwater environments (Whiticar et al. 1986). The shift in the $\delta^{13}\text{C}$ signature of moretene is interpreted as a shift in the bacterial community towards a higher proportion of methanotrophic bacteria similar to assemblages present in the modern lake.

Conclusions

At modern Lake Tswaing, the abundant higher-plant species characteristically produce odd-numbered long-chain n -alkanes ($n\text{-C}_{27,29,31,33}$), stigmaterol, β -sitosterol, β -amyirin, α -amyirin, lupeol and germanicol, as well as even-numbered long-chain alcohols ($n\text{-C}_{28,30}$). The floating cyanobacteria and microbial mats contain predominantly the C_{17} n -alkane, tetrahymanol and several C_{29} sterols. In the modern lake sediments, a mixture of these compounds is detected, together with phytane, phytene and the rare biomarker moretene, which point to an active bacterial community in the deeper lake or surface sediments. Bulk and compound-specific stable carbon isotope analyses give a more detailed picture of the modern carbon cycle of the Tswaing ecosystem, to which C3 and C4 plants and aquatic organisms contribute. Moretene thereby shows a distinctly lower isotopic composition than the other biomarkers, indicating the presence of methanotrophic bacteria.

The $\delta^{13}\text{C}$ signature of biomarkers identified in the modern ecosystem and their relative contribution to a 7-m long core sequence reveal changes in the ecosystem of the Tswaing Crater between 14,000 and 2,000 years BP. Under more humid conditions during Termination I (ca. 14,000–10,000 years BP), OM was almost absent in the sediments and was probably oxidised, whereas it was well preserved in a stagnant, saline lake environment afterwards. After a period of increased aquatic productivity at the

beginning Holocene, surface and bottom-water bi-productivity broke down between 10,000 and 7,500 years BP. This interval is interpreted to represent an arid period or a period with a long dry season, during which grasses and macrophytes were reduced around the lake and diminished nutrient input limited the aquatic bioproductivity. We propose a northward shift of the ITCZ to be the underlying forcing factor, which is in agreement with other African climate studies. After ca. 7,500 years BP, input from aquatic organisms increased with increasing humidity, reaching a maximum ca. 5,500 years BP. Microbial activity in particular was higher after ca. 7,500 years BP when methanotrophic bacteria seem to become an abundant constituent of the microbial lake community.

For the first time to our knowledge, long-chain alkenones (LCAs) were identified in African lake sediments. All samples containing LCAs are older than ca. 7,500 years BP and the occurrence of LCAs appears to reflect a different microbial community within the lake, indicated by up to 20‰ higher $\delta^{13}\text{C}$ values of moretene during that time period. Due to the unusual dominance of C_{38} LCAs and of tri- over tetra-unsaturated compounds, different source organisms than those described to date from other lake sites must be considered for Lake Tswaing.

Acknowledgments We acknowledge the GFZ for funding this work and for the financial support for the coring campaign in 2001/2002. We especially thank Susanne Fietz for investigating pigments in the cyanobacterial samples and Kai Mangelsdorf, Philippe Schaeffer, and Yannick Garcin for fruitful discussions. Carsten Löser is thanked for his help in botanical issues. We are grateful to Anke Sobotta, Cornelia Karger, Kristin Günther, Jenny Wunger und Michael Gabriel for technical help in the laboratories.

References

- Ashton PJ (1999) Limnology of the Pretoria Saltpan crater lake. In: Partridge TC (ed) Tswaing, investigations into the origin, age and palaeoenvironments of the Pretoria Saltpan. Council of Geoscience (Geological Survey of South Africa), Pretoria, pp 72–90
- Bligh EG, Dyer WJ (1959) A rapid method for total lipid extraction and purification. *Can J Biochem Physiol* 37:911–917
- Blumenberg M, Seifert R, Kasten S, Bahlmann E, Michaelis W (2009) Euphotic zone bacterioplankton sources major sedimentary bacteriohopanepolyols in the Holocene Black Sea. *Geochim Cosmochim Acta* 73:750–766
- Boon JP, Hines H, Burlingame AL, Klok J, Rijpstra WIC, De Leeuw JW, Edmunds KE, Eglinton G (1983) Organic geochemical studies of solar lake laminated cyanobacterial mats. In: Bjørøy M, Albrecht P, Cornford C, Groot KD, Eglinton G, Galimov E, Leythaeuser D, Pelet R, Rullkötter J, Speers G (eds) *Advances in organic geochemistry 1981*. Wiley, Chichester, pp 207–227
- Bühmann D, Elsenbroek JH (1999) Mineralogy and geochemistry of the Pretoria Saltpan borehole core. In: Partridge TC (ed) Tswaing, investigations into the origin, age and palaeoenvironments of the Pretoria Saltpan. Council of Geoscience (Geological Survey of South Africa), Pretoria, pp 91–117
- Castañeda IS, Werne JP, Johnson TC (2007) Wet and arid phases in the southeast African tropics since the last glacial maximum. *Geology* 35:823–826
- Collister JW, Rieley G, Stern B, Eglinton G, Fry B (1994) Compound-specific $\delta^{13}\text{C}$ analyses of leaf lipids from plants with differing carbon dioxide metabolisms. *Org Geochem* 21:619–627
- Cruz FW Jr, Burns SJ, Karmann I, Sharp WD, Vuille M, Cardoso AO, Ferrari JA, Silva Dias PL, Viana O Jr (2005) Insolation-driven changes in atmospheric circulation over the past 116,000 years in subtropical Brazil. *Nature* 434:63–66
- de Mesmay R (2008) Fonctionnement biogéochimique du Lac Masoko (Tanzanie), approche par les biomarqueurs lipidiques sédimentaires. PhD thesis, Université de la Méditerranée, p 122
- Eglinton G, Hamilton JE (1963) The distribution of alkanes. In: Swaine T (ed) *Chemical plant taxonomy*. Academic Press, New York, pp 187–217
- EPICA Community Members (2006) One-to-one coupling of glacial climate variability in Greenland and Antarctica. *Nature* 444:195–198
- Ficken KJ, Street-Perrott FA, Perrott RA, Swain DL, Olago DO, Eglinton G (1998) Glacial/interglacial variations in carbon cycling revealed by molecular and isotope stratigraphy of Lake Nkunga, Mt. Kenya, East Africa. *Org Geochem* 29:1701
- Ficken KJ, Wooller MJ, Swain DL, Street-Perrott FA, Eglinton G (2002) Reconstruction of a subalpine grass-dominated ecosystem, Lake Rutundu, Mount Kenya: a novel multiproxy approach. *Palaeogeogr Palaeoclimatol Palaeoecol* 177:137–149
- Fleitmann D, Burns SJ, Mudelsee M, Neff U, Kramers J, Mangini A, Matter A (2003) Holocene forcing of the Indian monsoon recorded in a stalagmite from southern Oman. *Science* 300:1737–1739
- Garcin Y, Vincens A, Williamson D, Buchet G, Guiot J (2007) Abrupt resumption of the African monsoon at the younger Dryas-Holocene climatic transition. *Quat Sci Rev* 26:690–704
- Gasse F (2000) Hydrological changes in the African tropics since the last glacial maximum. *Quat Sci Rev* 19:189–211
- Grimalt JO, Yruela I, Saiz-Jimenez C, Toja J, de Leeuw JW, Albaiges J (1991) Sedimentary lipid biogeochemistry of an hypereutrophic alkaline lagoon. *Geochim Cosmochim Acta* 55:2555–2577
- Grossi V, Baas M, Schogt N, Klein Breteler WCM, de Leeuw JW, Rontani JF (1996) Formation of phytadienes in the water column: myth or reality? *Org Geochem* 24:833–839

- Grossi V, Hirschler A, Raphel D, Rontani JF, de Leeuw JW, Bertrand JC (1998) Biotransformation pathways of phytol in recent anoxic sediments. *Org Geochem* 29:845–861
- Harvey HR, McManus GB (1991) Marine ciliates as a widespread source of tetrahymanol and hopan-3 β -ol in sediments. *Geochim Cosmochim Acta* 55:3387–3390
- Holmgren K, Lee-Thorp JA, Cooper GRJ, Lundblad K, Partridge TC, Scott L, Sithaldeen R, Siep Talma A, Tyson PD (2003) Persistent millennial-scale climatic variability over the past 25,000 years in southern Africa. *Quat Sci Rev* 22:2311–2326
- Hornibrook ERC, Longstaffe FJ, Fyfe WS, Bloom Y (2000) Carbon-isotope ratios and carbon, nitrogen and sulfur abundances in flora and soil organic matter from a temperate-zone bog and marsh. *Geochem J* 34:237–245
- Kleemann G, Poralla K, Englert G, Kjosien H, Liaaen-Jensen S, Neunlist S, Rohmer M (1990) Tetrahymanol from the phototrophic bacterium *Rhodospseudomonas palustris*: first report of a gammacerane triterpene from a prokaryote. *J Gen Microbiol* 136:2551–2553
- Kristen I, Fuhrmann A, Thorpe J, Röhl U, Wilkes H, Oberhänsli H (2007) Hydrological changes in southern Africa over the last 200 ka as recorded in lake sediments from the Tswaing impact crater. *S Afr J Geol* 110:311–326
- Larimer FW, Chain P, Hauser L, Lamerdin J, Malfatti S, Do L, Land ML, Pelletier DA, Beatty JT, Lang AS, Tabita FR, Gibson JL, Hanson TE, Bobst C, Torres JLT, Peres C, Harrison FH, Gibson J, Harwood CS (2003) Complete genome sequence of the metabolically versatile photosynthetic bacterium *Rhodospseudomonas palustris*. *Nat Biotechnol* 22:55–61
- Leng MJ, Lamb AL, Heaton THE, Marshall JD, Wolfe BB, Jones MD, Holmes J, Arrowsmith C (2005) Isotopes in lake sediments. In: Leng MJ (ed) *Isotopes in palaeoenvironmental research*. Springer, Dordrecht, pp 147–184
- Levi C, Labeyrie L, Bassinot F, Guichard F, Cortijo E, Waelbroeck C, Caillon N, Duprat J, de Garidel-Thoron T, Elderfield H (2007) Low-latitude hydrological cycle and rapid climate changes during the last deglaciation. *Geochem Geophys Geosys* 8(5):1–11. doi:10.1029/2006GC001514
- Li J, Philp RP, Pu F, Allen J (1996) Long-chain alkenones in Qinghai Lake sediments. *Geochim Cosmochim Acta* 60:235–241
- McCarthy RD, Duthie AP (1962) Rapid quantitative method for separation of free fatty acids from other lipids. *J Lipid Res* 3:117–119
- McCormac FG, Hogg AG, Blackwell PG, Buck CE, Higham TFG, Reimer PJ (2004) SHCal04 southern hemisphere calibration 0–11.0 cal k years BP. *Radiocarbon* 46:1087–1092
- O'Connor PW, Thomas DSG (1999) The timing and environmental significance of late quaternary linear dune development in western Zambia. *Quat Res* 52:44–55
- O'Leary MH (1981) Carbon isotope fractionation in plants. *Phytochemistry* 20:553–567
- Partridge TC (1999) Tswaing, investigations into the origin, age and palaeoenvironments of the Pretoria Saltpan. Council for Geosciences, Geological Survey of South Africa, Pretoria, p 198
- Partridge TC, deMenocal PB, Lorentz SA, Paiker MJ, Vogel JC (1997) Orbital forcing of climate over South Africa: a 200,000-year rainfall record from the Pretoria Saltpan. *Quat Sci Rev* 16:1125–1133
- Pearson EJ, Farrimond P, Juggins S (2007) Lipid geochemistry of lake sediments from semi-arid Spain: relationships with source inputs and environmental factors. *Org Geochem* 38:1169–1195
- Radke M, Sittard HG, Welte DH (1978) Removal of soluble organic matter from rock samples with a flow-through extraction cell. *Anal Chem* 50:663–665
- Radke M, Wilsch H, Welte DH (1980) Preparative hydrocarbon group type determination by automated medium pressure liquid chromatography. *Anal Chem* 52:406–411
- Reimer PJ, Baillie MGL, Bard E, Bayliss A, Beck JW, Bertrand C, Blackwell PG, Buck CE, Burr G, Cutler KB, Damon PE, Edwards RL, Fairbanks RG, Friedrich M, Guilderson TP, Hughen KA, Kromer B, McCormac FG, Manning S, Bronk Ramsey C, Reimer RW, Remmele S, Southon JR, Stuiver M, Talamo S, Taylor FW, van der Plicht J, Weyhenmeyer CE (2004) INTCAL04 terrestrial radiocarbon age calibration, 0–26 cal k years BP. *Radiocarbon* 46:1029–1058
- Rontani J-F, Volkman JK (2003) Phytol degradation products as biogeochemical tracers in aquatic environments. *Org Geochem* 34:1–35
- Rontani J-F, Volkman JK (2005) Lipid characterization of coastal hypersaline cyanobacterial mats from the Camargue (France). *Org Geochem* 36:251–272
- Rosenfeld WD, Silverman SR (1959) Carbon isotope fractionation in bacterial production of methane. *Science* 130:1658–1659
- Sakata S, Hayes JM, McTaggart AR, Evans RA, Leckrone KJ, Togasaki RK (1997) Carbon isotopic fractionation associated with lipid biosynthesis by a cyanobacterium: relevance for interpretation of biomarker records. *Geochim Cosmochim Acta* 61:5379–5389
- Schouten S, Hartgers WA, Lopez JF, Grimalt JO, Sinninghe Damsté JS (2001) A molecular isotopic study of ¹³C-enriched organic matter in evaporitic deposits: recognition of CO₂-limited ecosystems. *Org Geochem* 32:277–286
- Scott L (1999) Palynological analysis of the Pretoria Saltpan (Tswaing crater) sediments and vegetation history in the bushveld savanna biome, South Africa. In: Partridge TC (ed) *Tswaing, investigations into the origin, age and palaeoenvironments of the Pretoria Saltpan*. Council of Geoscience (Geological Survey of South Africa), Pretoria, pp 143–166
- Scott L (2002) Grassland development under glacial and interglacial conditions in southern Africa: review of pollen, phytolith and isotope evidence. *Palaeogeogr Palaeoclimatol Palaeoecol* 177:47–57
- Scott L, Holmgren K (2003) Age interpretation of the Wonderkrater spring sediments and vegetation change in the savanna biome, Limpopo province, South Africa. *S Afr J Sci* 99:484–488
- Street-Perrott FA, Ficken KJ, Yongsong H, Eglinton G (2004) Late quaternary changes in carbon cycling on Mt. Kenya, East Africa: an overview of the $\delta^{13}\text{C}$ record in lacustrine organic matter. *Quat Sci Rev* 23:861–879
- Sun Q, Chu G, Liu G, Li S, Wang X (2007) Calibration of alkenone unsaturation index with growth temperature for a lacustrine species, *Chysothila lamellosa* (Haptophyceae). *Org Geochem* 38:1226–1234

- Talbot MR, Lærdal T (2000) The late Pleistocene-Holocene palaeolimnology of Lake Victoria, East Africa, based upon elemental and isotopic analyses of sedimentary organic matter. *J Paleolimnol* 23:141–164
- Thiel V, Jenisch A, Landmann G, Reimer A, Michaelis W (1997) Unusual distributions of long-chain alkenones and tetrahymanol from the highly alkaline lake Van, Turkey. *Geochim Cosmochim Acta* 61:2053–2064
- Tissot BP, Welte DH (1984) Petroleum formation and occurrence. Springer, Berlin
- Tornabene TG, Langworthy TA, Holzer G, Oró J (1979) Squalenes, phytanes and other isoprenoids as major neutral lipids of methanogenic and thermoacidophilic “archaeobacteria”. *J Mol Evol* 13:73–83
- Uemura H, Ishiwatari R (1995) Identification of unusual 17[β](H)-moret-22(29)-ene in lake sediments. *Org Geochem* 23:675–680
- Volkman JK (2005) Sterols and other triterpenoids: source specificity and evolution of biosynthetic pathways. *Org Geochem* 36:139–159
- Wang X-C, Chen RF, Berry A (2003) Sources and preservation of organic matter in Plum Island salt marsh sediments (MA, USA): long-chain *n*-alkanes and stable carbon isotope compositions. *Estuar Coast Shelf Sci* 58:917–928
- Whiticar MJ, Faber E, Schoell M (1986) Biogenic methane formation in marine and freshwater environments: CO₂ reduction vs. acetate fermentation—*isotope evidence*. *Geochim Cosmochim Acta* 50:693–709
- Wooller MJ, Swain DL, Ficken KJ, Agnew ADQ, Street-Perrott FA, Eglinton G (2003) Late quaternary vegetation changes around Lake Rutundu, Mount Kenya, East Africa: evidence from grass cuticles, pollen and stable carbon isotopes. *J Quat Sci* 18:3–15
- Wooller MJ, Zazula GD, Edwards M, Froese DG, Boone RD, Parker C, Bennett B (2007) Stable carbon isotope compositions of eastern Beringian grasses and sedges: investigating their potential as paleoenvironmental indicators. *Arct Antarct Alp Res* 39:318–331
- Zink K-G, Leythaeuser D, Melkonian M, Schwark L (2001) Temperature dependency of long-chain alkenone distributions in recent to fossil limnic sediments and in lake waters. *Geochim Cosmochim Acta* 65:253–265